SNS WARM LINAC COMMISSIONING RESULTS *

A. Aleksandrov on behalf of the SNS collaboration, Spallation Neutron Source,
Oak Ridge National Laboratory, Oak Ridge, TN 37830 USA

Abstract

The Spallation Neutron Source accelerator systems will deliver a 1.0 GeV, 1.4 MW proton beam to a liquid mercury target for neutron scattering research. The staged beam commissioning of the accelerator complex is proceeding as component installation progresses. The Front End, Drift Tube Linac and three of the four Coupled-Cavity Linac modules have been commissioned with beam at ORNL. Results and status of the beam commissioning program are presented.

INTRODUCTION

The accelerator complex consists of an H^- injector, capable of producing one-ms-long pulses with 38 mA peak current, chopped with a 68% beam-on duty factor and repetition rate of 60 Hz to produce 1.6 mA average current, a 1 GeV linear accelerator, an accumulator ring, and associated transport lines [1]. The 2.5 MeV beam from the Front End is accelerated to 86 MeV in the Drift Tube Linac, then to 185 MeV in a Coupled-Cavity Linac and finally to 1 GeV in the Superconducting Linac. The staged beam commissioning of the accelerator complex is proceeding as component installation progresses. At this point, the H^- injector (Front End), Drift Tube Linac and Coupled Cavity Linac modules 1, 2 and 3 (of 4) have been commissioned at ORNL. A comparison of major beam design parameters with the parameters achieved during commissioning is shown in Table 1.

FRONT-END PERFORMANCE

The front-end for the SNS accelerator systems is a 2.5 MeV injector consisting of the following major subsystems: an rf-driven H^- source, an electrostatic low energy beam transport line (LEBT), a 402.5 MHz RFQ, a medium energy beam transport line (MEBT), a beam chopper system and a suite of diagnostic devices. The front-end is required to produce a 2.5 MeV beam of 38mA peak current at 6% duty factor. The 1 ms long H^- macro-pulses are chopped at the revolution frequency of the accumulator ring (~1 MHz) into mini-pulses of 645 ns duration with 300 ns gaps. The front-end has been providing beam for commissioning the rest of the linac since the initial commissioning at the SNS site in 2002. More than 2500 hours of operation time have been accumulated so far, and commissioning goals have been achieved and results published in [2]. This paper reports the most recent achievements only.

* SNS is managed by UT-Battelle, LLC, under contract DE-AC05-00OR22725 for the U.S. Department of Energy. SNS is a partnership of six national laboratories: Argonne, Brookhaven, Jefferson, Lawrence Berkeley, Los Alamos and Oak Ridge.

Ion Source and LEBT Performance

Details of the ion source and LEBT design can be found in [3]. A maximum current of 51 mA was achieved, significantly exceeding the base line requirement of 38 mA. An R&D program on the ion-source hot spare stand [4] yielded a significant increase of the ion source availability: starting at 85.6%, it increased to 92.4% in the second, and finally to 98.6% in the most recent run.

Table 1. SNS achieved vs. design beam parameters.

Parameter	Design	Achieved
Peak current [mA]	38	>38
Average current [mA]	1.6	1.05 DTL1 run 0.002 CCL run
H^-/pulse [$x10^{14}$]	1.6	1.3 DTL1 run 0.1 CCL run
Pulse length [msec]/Rep-rate [Hz]/Duty Factor [%]	1.0/60/6	1.0/60/3.8 DTL1 .05/1/.005 CCL
MEBT rms emittance, normalized [π mm mrad]	0.3	< 0.3 horizontal and vertical
DTL1 rms emittance, normalized [π mm mrad]	0.3	0.4 horizontal 0.3 vertical
DTL6 rms emittance, normalized [π mm mrad]	0.3	0.32 horizontal 0.39 vertical
MEBT bunch length, rms [degrees of 402.5 MHz]	18.5	18
CCL1 bunch length, rms [degrees of 805 MHz]	2.8	7.4
Max output energy [MeV]	157.2	158.08±0.40

RFQ Performance

The design of the 3.72 m-long 4-vane RFQ with π-mode stabilizers is described in detail elsewhere [5]. It operates at 402.5 MHz and accelerates the H^- beam from 65 kV to 2.5 MeV.

We were not able to measure the beam current injected into the RFQ from the LEBT, therefore an estimation of the RFQ transmission of ~90 % is obtained by comparing the measured output current vs. RF power curve with the PARMTEQH simulations (see Fig. 1).

The RFQ output energy was measured by a time-of-flight technique in the MEBT and found to be 2.45±0.01 MeV, compared with the 2.5 MeV nominal design energy.

The Twiss parameters of the RFQ output beam were measured using the wire scanners in the MEBT. There is good agreement with the design values in the horizontal plane but the vertical beta-function is smaller than expected by about factor of 2 (see Fig.2).

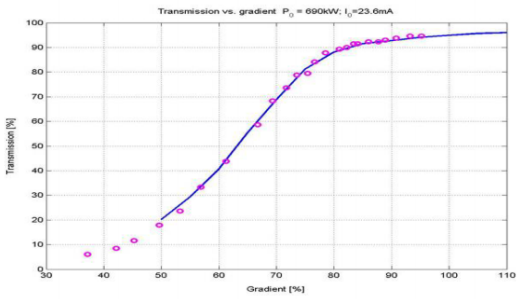

Figure 1. RFQ transmission vs. RF power. Measurements (red) and model fit (blue) .

MEBT Performance

The MEBT is a complex beam transport line [6]. It matches the beam from the RFQ through the MEBT chopper system and into the drift-tube linac. Fourteen quadrupole magnets and four bunching cavities provide transverse and longitudinal focusing. The MEBT is equipped with a suite of beam diagnostics [7] including two beam current monitors (BCM), six beam position and phase monitors (BPM), and five dual- plane wire scanners (WS). A dual plane slit/collector type emittance device and a 3-d profile measurement system utilizing a mode-locked laser were added recently. Part of the laser transport system providing the longitudinal measurements was commissioned during the last run. A set of two horizontal scrapers was installed in the middle of the MEBT for halo mitigation study proposed in [8].

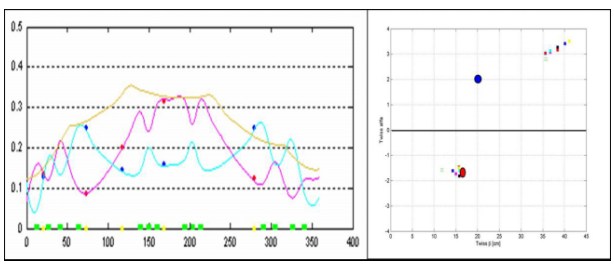

Figure 2. Left: Beam profile (cm) vs. distance in the MEBT (cm). The points show measured horizontal and vertical beam profiles and the curves show the predicted horizontal profile (red), vertical profile (blue) and longitudinal profile (brown). Right: RFQ output Twiss parameters, design (large circles) and measured (squares)

The beam trajectory can be easily corrected to less than 1 mm offset in the BPMs and there are no measurable losses within the accuracy of the BCMs when quadrupoles are set to the design strengths.

Comparison of the design beam size with the wire scanner measurements in Fig. 2 shows good agreement when the MEBT input Twiss parameters in the model are adjusted to best fit the measurements. The wire scans and the model fit were done for a set of different quadrupole settings in the MEBT, producing a set of the input Twiss parameters, shown in Fig. 2 by squares. There is a spread of calculated values due to the measurement errors and model simplifications but the observed discrepancy in the vertical plane (blue circle) is significantly larger than the spread and the possible cause is still being investigated.

The transverse phase space measured at 2/3 of the MEBT length is shown in Fig. 3. The emittance values are within the design requirements (see Table 1.). The effect of the scraper can be clearly seen in Fig. 3. The left picture shows significant halo, which is removed by a pair of scrapers at a single location. This measurement confirms the correct choice of the scraper location.

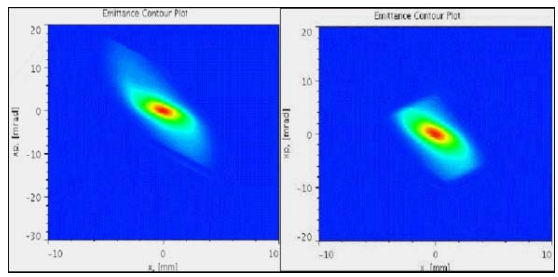

Figure 3 Beam transverse phase space in the MEBT with scraper out (left) and in (right).

The longitudinal bunch profiles measured with the mode-locked laser system are shown in Fig. 4. The bunch has a symmetric Gaussian-like profile when the upstream rebuncher phase is set correctly (bottom left). When the rebuncher phase is off from the nominal a head to tail asymmetry appears (top left and right) in good agreement with the simulation. The rms bunch length vs. the rebuncher phase is shown at bottom right. The measured values (squares) are in good agreement with the PARMILA prediction (stars). This measurement confirms that longitudinal bunch parameters are close to the design.

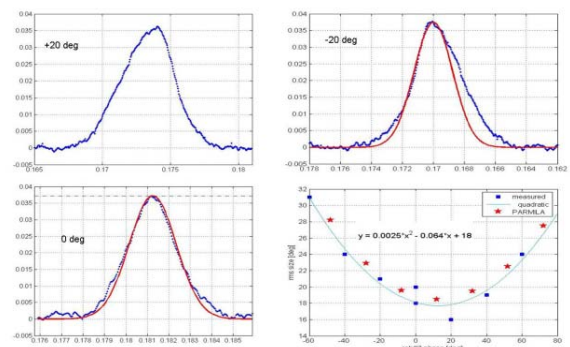

Figure 4. Longitudinal bunch profile measured with mode-locked laser in the MEBT (blue dots) and Gaussian fit (red line).Bottom right: rms bunch length vs. the rebuncher phase (measurements – squares, simulation – stars, solid line – quadratic fit).

Chopping

The 1-ms long H^- macro-pulses have to be chopped at the revolution frequency of the accumulator ring into mini-pulses of 645 ns duration with 300 ns gaps. Beam chopping is performed by two separate chopper systems located in the LEBT and MEBT. The LEBT chopper removes most of the beam charge during the mini-pulse gaps, and the traveling-wave MEBT chopper further

cleans the gap and reduces the rise and fall time of the mini-pulse to 10 ns. The last lens in the LEBT is split into four quadrants to allow electrostatic chopping using the RFQ entrance flange as a chopper target. The MEBT chopper attenuates the beam in the gap to a level of 10^{-4} [9]. Chopped patterns produced by the LEBT and MEBT choppers in the beam were measured using a Faraday cup and fast oscilloscope (see Fig. 5). Single 600 ns mini-pulse (one turn in the ring) and nominal duty factor modes were demonstrated (top right and left, respectively). The bottom plot in Fig. 5 demonstrates shortening of the beam rise time due to the MEBT chopper (blue line) in addition to the LEBT chopper alone (green line). The oscilloscope resolution did not allow an extinction ratio measurement to the design level of 10^{-4}. A laser based system capable of measuring rise/fall times with 5 ns resolution and a beam extinction ratio with 10^{-4} resolution has been developed and tested [10]. It's expected to become available during the SCL commissioning run.

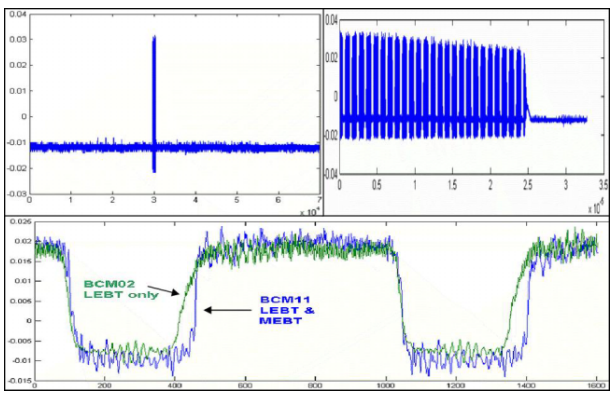

Figure 5. The chopped beam patterns: single turn (top left) and the nominal duty factor (top right). The beam rise time with the LEBT chopper alone (green) and with the MEBT chopper added (blue).

DRIFT TUBE LINAC PERFORMANCE

The Drift Tube Linac consists of six accelerating tanks operating at 402.5 MHz with final output energy of 87 MeV. The transverse focusing is arranged in a FFODDO lattice utilizing permanent-magnet quadrupoles. Some empty drift tubes contain BPMs and dipole correctors. The inter-tank sections contain BCMs, wire scanners and energy degrader/faraday cups (ED/FC).

The DTL tanks have been commissioned with beam in three separate runs. One of these runs included a high power beam test.

High power beam test

In the first run, DTL tank 1 (with output energy 7.5 MeV) was commissioned using a high-power beam collector for a test of high-power operation. The design peak current of 38 mA was readily achieved. A 1-msec long beam pulse was generated at 20 mA average current during the pulse (at low duty factor). Finally, a 1 mA average current beam was accelerated in DTL1 with 100% beam transmission. For this demonstration, a beam pulse of 26 mA peak current, 650 microsecond pulse length at 60 Hz (7.6 kW beam power) was achieved. Fig. 6 shows an overlay of Beam Current Monitor signals in the MEBT and DTL1 during this high-power demonstration run. This was an important milestone, in that it shows the injector and DTL1 is capable of 1 MW-class SNS operation.

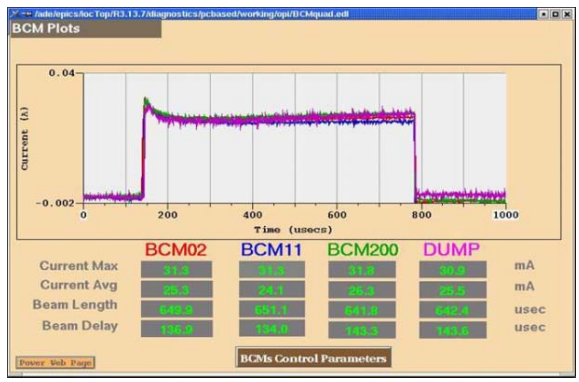

Figure 6. Beam pulse the MEBT and DTL1 during the high beam power test.

DTL tuning and performance

In all subsequent commissioning runs a low-power beam stop was used. It limited the beam pulse lengths to less than 50 microseconds, and repetition rates to 1 Hz.

We used two procedures for setting the RF phase and amplitude of the DTL tanks. In the first one, the so called the acceptance scan, the tank transmission vs. the RF phase curve is measured and the width of the acceptance window is compared with the model. The degrader thickness of the ED/FCs located after each tank is chosen to absorb beam particles with energy below the design energy. A screen snapshot of a typical scan is shown in Fig. 7.

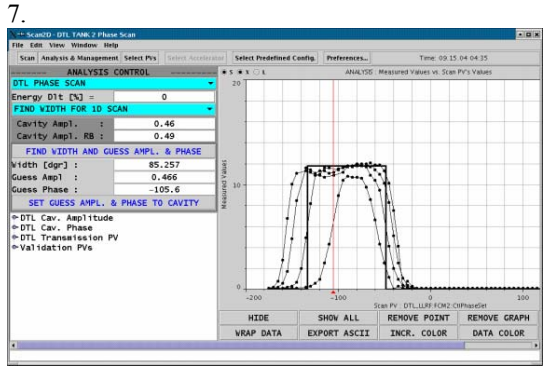

Figure 7. Acceptance scan of the DTL tank1. The current transmitted through the degrader is measured on the Faraday cup as a function of DTL1 phase at different RF amplitudes. Solid rectangle shows acceptance width determined by the software for a particular amplitude.

The second technique is based on the "phase-scan signature matching" approach [11], where the beam phase from a single BPM, or the phase difference between two BPMs downstream of a DTL tank, are measured as a function of the tank phase and amplitude and compared

with the model (the XAL implementation of the algorithm is dubbed PASTA [12]). Figure 10 shows an example of a scan for DTL tank 1, in which three sets of beam phase vs. tank phase were measured. One scan was taken at nominal RF amplitude, one at 5% above nominal, and the other at 5% below. As the plots show, the signatures are quite sensitive to the RF amplitude. A model-based fit was then performed to three phase-scan "signatures" simultaneously to obtain the RF amplitude, relative phase of the beam and RF, and the input energy.

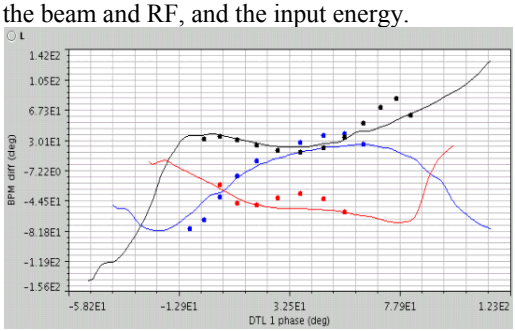

Figure 8. Curves show the measured phase difference (degrees) between two BPMs downstream of DTL1 as functions of DTL1 RF phase for nominal RF amplitude (blue), 5% below nominal (red) and 5% above nominal (black). The points show the result of a model-based fit to the data.

There is a good agreement between the two methods [12]. PASTA has the advantage of using non-interceptive BPMs. In contrast, the beam pulse width and current had to be reduced when inserting the ED/FCs for the acceptance scan procedure.

An estimate of the energy jitter and long-term drift was done by averaging BPM phase data taken during a 30-minute periods. Typical rms output energy spread is 0.08%, which corresponds to 0.6 degrees phase spread measured on a single BPM.

Transverse matching between the MEBT and the DTL is achieved by adjusting strengths of the four last quadrupoles in the MEBT. The optimal settings were close to the design values but we found less sensitivity of the beam profile tails to a mismatch than was predicted by the simulations [13].

COUPLED CAVITY LINAC

The Coupled Cavity Linac (CCL) consists of four 12-segment accelerating modules operating at 805 MHz with final output energy of 186 MeV. The inter-segment sections contain electromagnet quadrupoles arranged in a FODO focusing lattice, BPMs, wire scanners and Beam Shape Monitors [14].

CCL modules 1,2 and 3 have been commissioned.

CCL tuning and performance

The main procedure for setting the RF phase and amplitude of the CCL modules relies on the so-called delta-T scan. The phase from a pair of BPMs downstream of the CCL modules is measured for different RF phases. The RF phase and amplitude set points can be derived from measurements and model predictions [15]. The PASTA software was also tried and good agreement between the two methods was observed [12].

After tuning the warm linac at low (~15 mA) current we encountered difficulties in transporting higher currents due to the beam loading effect. As seen on the LLRF system screen snapshot in Fig. 9, there is a significant cavity field and phase droop during the beam pulse transient. Apparently, the LLRF bandwidth is not wide enough to compensate for the beam loading when working with short pulses. The detrimental effect on the beam dynamics is shown in Fig. 10, where the bunch width along the pulse measured by the BSM in the CCL is shown. The beam loading leads to significant variation of the average bunch phase within the pulse (left picture). An adaptive feed forward compensation was added to the LLRF system [16]. As a result, the cavity field droop was flattened out (right plot in Fig. 9) and the beam phase became uniform along the bunch (right picture in Fig. 10).

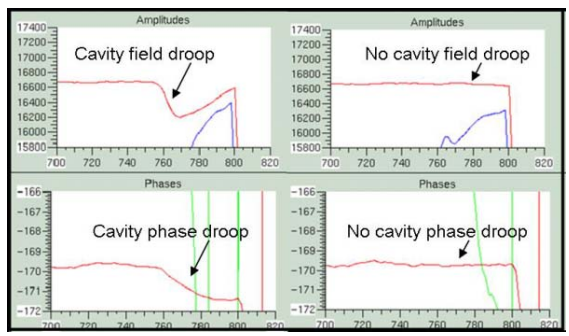

Figure 9. Cavity field and phase droop with feedback alone (left) and feedback + feedforward (right) beam loading compensation.

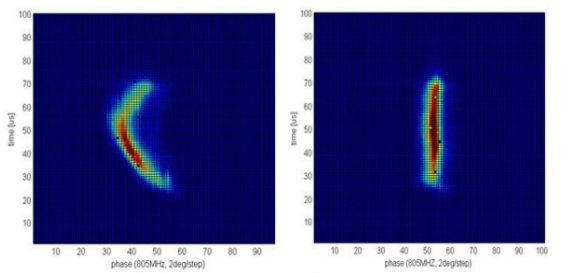

Figure 10. Phase width of the bunch (x axis) along the pulse (y axis) with feedback alone (left) and feedback + feedforward (right) beam loading compensation.

With an addition of the feed forward compensation a nominal peak current of 38 mA was readily transported through the warm linac with 100% transmission (within the 1-3% BCM measurement uncertainty) as illustrated in Fig. 11.

Time-of-flight energy measurements after the DTL-6 and CCL 1-3 were performed using several pairs of BPMs located in the CCL. Results are shown in Table 2. The measured beam energy is in good agreement with the design values.

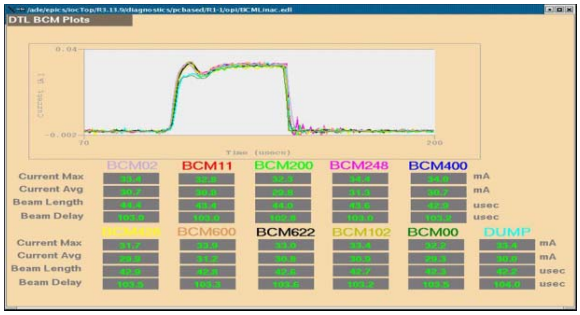

Figure 11. Beam current monitor traces show the beam current after the RFQ, after the MEBT, after the DTL1, 2, 3, 4, 5, 6, after the CCL3, and at the beamstop.

Table 2 Beam energy from time-of-flight measurements

Output of	Design [MeV]	Measured [MeV]	Deviation [%]
DTL6	86.83	87.48±0.03	0.75
CCL1	107.16	107.36±0.12	0.19
CCL2	131.14	131.53±0.14	0.40
CCL3	157.21	158.08±0.40	0.55

The bunch profiles measured at three locations in the CCL-1 using the BSM are shown in Fig 12. They have Gaussian-like shapes without significant tails but the rms width is significantly larger than expected from the simulations. The plot on bottom right in Fig. 12 shows all available experimental data taken with different linac tunes at different currents (asterisks) and the bunch width predicted by the PARMILA (stars). There is factor of 2-3 difference even in the best case. Unfortunately, we discovered this discrepancy during the data analysis after the beam run was finished and couldn't conduct additional experimental study. Possible explanations of the problem are discussed in [13]. Further experimental study is planned for the next beam run.

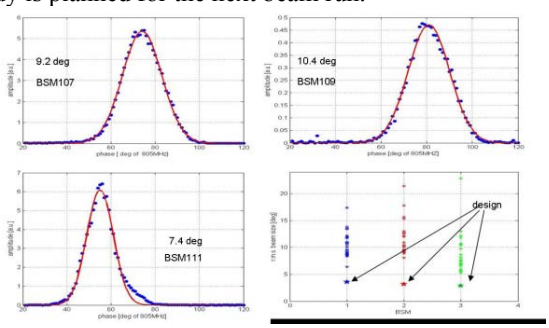

Figure 12. Longitudinal bunch profile measured at three BSM stations in the CCL1 (dots) and Gaussian fit (solid line) . Bottom rigth graph shows rms bunch width for all measurements (asterisks) and design values (stars).

Transverse matching between the DTL and CCL is achieved by adjusting strengths of the four quadrupoles in the beginning of the CCL. We found that only minor adjustments were required to achieve a good match judged by beam profile shapes in the CCL. Discussion of the measurements can be found in [17]. There is no measurable beam loss in the linac when the optimal matching is achieved. Fig. 13 shows the distribution of the beam spill along the warm linac measured with BLMs. When the background is properly subtracted the remaining loss signal is associated with the beam stop after the CCL-4. We will be able to achieve a better sensitivity during the next run when the temporary beam stop is removed.

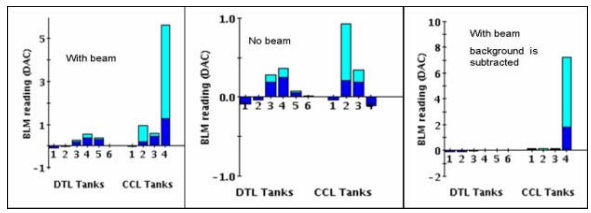

Figure 13. Beam loss distribution along the linac. Raw data with beam on (left), no beam (center), With beam on and subtracted background (right).

CONCLUSIONS

Commissioning of the SNS linac has been progressing well. Acceleration to the design energy of 157 MeV of beam pulses with the design peak current of 38 mA has been achieved. The Front End and DTL1 were operated at 1 mA average current. In general, there is good agreement between the measured beam parameters and the design values. The larger than expected bunch length in the CCL is the biggest discrepancy found so far, and the cause is under investigation. The CCL module 4 is the only part of the warm linac remaining to be commissioned. It has been RF conditioned to the design field level and will be commissioned at the beginning of the next beam run in summer 2005.

REFERENCES

[1] N. Holtkamp, Proc. PAC 2003, p. 11.
[2] A. Aleksandrov, Proc. PAC 2003, p.533
[3] R. Keller et al., in "9th Int. Symp. on the Production and Neutralization of Negative Ions and Beams". edited by M. Stockli, AIP Conf. Proc. No. 639, p. 47.
[4] R. Welton et al, in these proceedings.
[5] A. Ratti et al., Proc. EPAC 2000, p. 495.
[6] J. Staples et al., Proc. LINAC 2000, p. 250.
[7] S. Assadi , Proc. PAC 2003, p. 498.
[8] D. Jeon et. al., PRSTAB 5, 094201 (2002).
[9] R. Hardekopf et al., PAC 2004.
[10] A. Aleksandrov et al., PAC 2003, p. 1524.
[11] T. Owens et al., Part. Acc. **48** (1994), p. 169.
[12] J. Galamos et al., in these proceedings.
[13] S. Henderson et al., in these proceedings.
[14] A. Feshenko et al., Proc. LINAC 2004, p.408
[15] A. Feshenko et al., in these proceedings.
[16] M.Champion et al., in these proceedings.
[17] P. Chu et al., in these proceedings.